Development of highly potent glucocorticoids for steroid-resistant severe asthma

Yuanzheng He[a,b,1,2], Jingjing Shi[c,1], Quang Tam Nguyen[d,1], Erli You[c], Hongbo Liu[e], Xin Ren[f], Zhongshan Wu[g], Jianshuang Li[h], Wenli Qiu[f], Sok Kean Khoo[i], Tao Yang[h], Wei Yi[c,j,k,2], Feng Sun[g], Zhijian Xi[g], Xiaozhu Huang[f,3], Karsten Melcher[b], Booki Min[d,2], and H. Eric Xu[b,c,2]

[a]Laboratory of Receptor Structure and Signaling, HIT Center for Life Science, Harbin Institute of Technology, Harbin 150001, China; [b]Laboratory of Structural Sciences, Van Andel Research Institute, Grand Rapids, MI 49503; [c]Van Andel Research Institute–Shanghai Institute of Materia Medica, Center for Structure and Function of Drug Targets, Key Laboratory of Receptor Research, Shanghai Institute of Materia Medica, Chinese Academy of Sciences, Shanghai 201203, China; [d]Department of Inflammation and Immunity, Lerner Research Institute, Cleveland Clinic Foundation, Cleveland, OH 44195; [e]Center of Epigenetics, Van Andel Research Institute, Grand Rapids, MI 49503; [f]Department of Medicine, Lung Biology Center, University of California, San Francisco, CA 94158; [g]Department of Research and Development, Palo Alto Pharmaceuticals, Shanghai 201203, China; [h]Laboratory of Skeletal Biology, Van Andel Research Institute, Grand Rapids, MI 49503; [i]Department of Cell and Molecular Biology, Grand Valley State University, Grand Rapids, MI 49401; [j]Key Laboratory of Molecular Target and Clinical Pharmacology, School of Pharmaceutical Sciences, Guangzhou Medical University, Guangzhou, Guangdong 511436, China; and [k]State Key Lab of Respiratory Disease, Fifth Affiliated Hospital, Guangzhou Medical University, Guangzhou, Guangdong 511436, China

Edited by John A. Cidlowski, National Institutes of Environmental Health Sciences, Research Triangle Park, NC, and accepted by Editorial Board Member Ruslan Medzhitov February 22, 2019 (received for review September 28, 2018)

Clinical application of inhaled glucocorticoids (GCs) has been hampered in the case of steroid-resistant severe asthma. To overcome this limitation, we have developed a series of highly potent GCs, including VSGC12, VSG158, and VSG159 based on the structural insight into the glucocorticoid receptor (GR). Particularly, VSG158 exhibits a maximal repression of lung inflammation and is 10 times more potent than the currently most potent clinical GC, Fluticasone Furoate (FF), in a murine model of asthma. More importantly, VSG158 displays a unique property to reduce neutrophilic inflammation in a steroid-resistant airway inflammation model, which is refractory to clinically available GCs, including dexamethasone and FF. VSG158 and VSG159 are able to deliver effective treatments with reduced off-target and side effects. In addition, these GCs also display pharmacokinetic properties that are suitable for the inhalation delivery method for asthma treatment. Taken together, the excellent therapeutic and side-effect profile of these highly potent GCs holds promise for treating steroid-resistant severe asthma.

steroid-resistant asthma | glucocorticoid | high potency | VSG158 | VSG159

Asthma is a common chronic inflammatory disease that affects about 8% of the US population (1) and is characterized by airway obstruction and bronchospasm (2). Although asthma is caused by a combination of complex environmental and genetic factors, lung inflammation is the direct cause of airway obstruction and bronchospasm. Therefore, almost all asthma treatments focus on repressing or controlling lung inflammation, and glucocorticoids (GCs) are the most commonly used antiinflammation agents. Inhaled GCs were first introduced to asthma treatment in the early 1970s and revolutionized the management of patients with chronic asthma (3). Since then, inhaled GCs have become the most effective treatment of asthma. In particular, the combination of GCs (antiinflammatories) and β2-adrenergic receptor agonists (bronchial dilators) has been successful in preventing and controlling most cases of asthma attacks and has greatly lowered the death rate caused by asthma (4). However, the clinical application of inhaled GCs still encounters two major obstacles. First, patients with severe asthma respond poorly to inhaled GCs (referred to as "steroid resistance") (5). Second, long-term use of inhaled GCs still causes adverse effects, such as sore mouth (hoarseness), slight growth reduction for children, decreased bone mass and strength, and high blood pressure in adults (6, 7). Clinical studies have shown that highly potent GCs, such as Fluticasone Furoate (FF) and Fluticasone Propionate (FP), improve the lung function of a subset of patients with uncontrolled asthma (8, 9). Particularly, in combination with vilanterol, a long-acting β2-adrenergic receptor agonist, FF has been shown to improve the treatment adherence in certain patients with chronic obstructive pulmonary disease (COPD) (10), in which steroid resistance is the major barrier for effective treatment. Notably, highly potent GCs usually have a higher receptor binding ability and are generally associated with a fast acting time (11), which is important for relieving the asthma symptoms in certain life-threatening conditions such as severe asthma and COPD. Therefore, there is an unmet medical need for designing and developing highly potent GCs for asthma treatment.

Previously, our laboratory had determined the mechanism of GC potency through solving the structure of the GR ligand-binding domain (LBD) in complex with GCs of different potencies (12), including the highly potent Mometasone Furoate (MF). The

Significance

Severe asthma generally responds poorly to traditional steroid treatment and causes most of the disability and mortality among all asthma patients. Currently, there is almost no effective treatment to control the symptoms of severe asthma. Our insight into the structure of glucocorticoid (GC) potency has enabled us to develop GCs with maximal potency to repress lung inflammation in a murine model of asthma, outperforming the currently most effective clinical compound, and is capable of delivering a treatment with reduced off-target and side effects in many categories. Most importantly, the extremely potent GC VSG158 alleviates the inflammation response in a murine steroid-resistant airway inflammation model when leading clinical compounds fail, suggesting a therapeutic potential of these GCs for controlling severe asthma.

Author contributions: Y.H., T.Y., W.Y., X.H., K.M., B.M., and H.E.X. designed research; Y.H., J.S., Q.T.N., E.Y., H.L., X.R., Z.W., J.L., W.Q., and F.S. performed research; S.K.K. and Z.X. contributed new reagents/analytic tools; Y.H., B.M., and H.E.X. analyzed data; and Y.H. B.M., and H.E.X. wrote the paper.

Conflict of interest statement: F.S., Z.W., and Z.X. are employees and H.E.X. is a consultant of Palo Alto Pharmaceutics Inc.

This article is a PNAS Direct Submission. J.A.C. is a guest editor invited by the Editorial Board.

Data deposition: The data reported in this article have been deposited in the National Center for Biotechnology Information Gene Expression Omnibus database (accession no. GSE119789).

[1]Y.H., J.S., and Q.T.N. contributed equally to this work.

[2]To whom correspondence may be addressed. Email: ajian.he@hit.edu.cn, yiwei@gzhmu.edu.cn, minb@ccf.org, or eric.xu@vai.org.

[3]Deceased December 18, 2017.

This article contains supporting information online at www.pnas.org/lookup/suppl/doi:10.1073/pnas.1816734116/-/DCSupplemental.

Published online March 20, 2019.

MF-bound GR LBD structure revealed that the high potency of MF is achieved mainly by the furoate group at the C17-α position of the GC backbone fully occupying a hydrophobic cavity in the GR ligand-binding pocket. Utilizing this structural insight, we designed a highly potent GC, VSG22, which shows more than 1,000 times potency improvement over its backbone VSG24 (12). Further modification of VSG22 based on additional structural insight gained from the deacylcotivazol- and dexamethasone (DEX)-bound GR LBD structures has allowed us to generate another GC derivative, VSGC12, which shows superior antiinflammatory properties in in vitro assays (12, 13). In a mouse asthma model, VSGC12 shows a higher potency than intraperitoneally (i.p.) delivered FF and is able to provide the same treatment effect as FF at a dose that does not elicit significant side effects (14). Since high potency has been implicated in improving symptoms of severe asthma, we have further optimized VSGC12 in an attempt to reach the maximal potency for lung inflammation repression and lowering the systemic availability. Guided by this strategy, we have designed and developed a series of extremely potent GCs, including VSG158 and VSG159, that have a superior treatment effect in a murine model of asthma and deliver a treatment effect at a dose that does not evoke significant adverse effects. Even more exciting is that VSG158 is able to deliver a treatment effect in a mouse model of steroid-resistant airway inflammation, in which neither DEX nor FF have an effect. These extremely potent GCs may hold promise for asthma treatment, particularly for those patients with a severe or uncontrolled condition.

Results

Design and Development of Highly Potent GCs. FP is one of the most successful clinical GCs for asthma treatment due to its high potency and ideal pharmacokinetic properties (15, 16). A key advantage of FP is its extremely low oral bioavailability (1%), which minimizes systemic exposure of swallowed compound in the gastrointestinal (GI) tract during inhalation (17). The low oral bioavailability is due mainly to first-pass hepatic metabolism by the hydrolysis of the *S*-fluoromethyl carbothioate group from the C-21 position of FP. Previously, we generated VSGC12 based on additional structural clues on the C-6, C-9, and C16 positions of the GC backbone (14). VSGC12 shows a higher potency than FF by i.p. administration in a mouse asthma model; however, initial side-effect data suggested that VSGC12 has a relatively high systemic exposure after oral administration. VSGC12 has a nitro group at the C-21 position that cannot be hydrolyzed in the liver, which we suspect explains the high systemic exposure of VSGC12 after oral administration. Therefore, we decided to further optimize VSGC12, focusing on introducing a hydrolyzable group at the C-21 position (Fig. 1*A*), which generated a series of compounds (VSG155-161). Among those modifications, VSG155 has a hydroxyl group at the C-21 position, representing the hydrolyzed product of this series (except for VSG160, which is not hydrolyzable). As expected, VSG155 shows much less transactivation activity in a mouse mammary tumor virus (MMTV) luciferase reporter assay, particularly at the subsaturation dose of 10 nM (Fig. 1*B*). A transactivation dose–response curve shows that VSG158 has the highest potency among the series of newly designed compounds (Fig. 1*C*). In the transrepression dose–response curve, both VSG158 and VSG159 show a high potency in the AP1 luciferase repression assay, very similar to that of the FF compound (Fig. 1*D*). In a ^{3}H-DEX competition binding assay, both VSG158 and VSG159 show a stronger binding affinity than DEX; particularly, VSG158 has almost the same binding affinity to GR as FF (Fig. 1*E*), which has the highest reported affinity to GR (16, 18). It is worth noting that VSG158 and VSG159 have almost the same potency as FF in repression of AP-1, but show 10- to 20-fold less potency than FF in transactivation of MMTV-Luc, indicating the dissociation of these two GR activities of VSG158 and VSG159 (Fig. 1 *C* and *D*). Because most side effects of GCs are believed to be caused by their transactivation activities, the much less potent transactivation activities of VSG158 and VSG159 are a desired property.

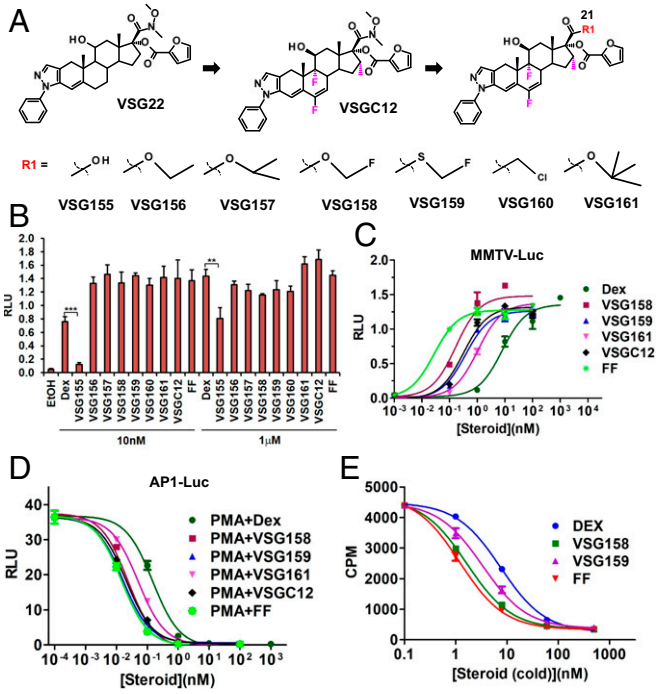

Fig. 1. In vitro activity of GCs. (*A*) Chemical structures of a series of GCs with modification of the C-21 position of VSGC12. (*B*) The transactivation activity of VSG155–161 on a MMTV-luciferase reporter in AD293 cells. (*C*) Dose–response curve of the transactivation activities of GCs on the MMTV-luciferase reporter in AD293 cells. (*D*) Dose–response curve of the transrepression activities of GCs on the AP1-luciferase reporter in AD293 cells. (*E*) In vitro ^{3}H-DEX competition binding assay of GCs; the Ki for FF, VSG158, VSG159, and DEX are 1.217, 1.659, 3.347, and 7.576 nM, respectively. Error bars indicate SD; $^{**}P < 0.01$; $^{***}P < 0.001$; one-way ANOVA analysis with a Tukey test; $n = 3$.

Off-Target Effects of GCs. GR belongs to the steroid hormone receptor subfamily of the nuclear receptor super family. Other members of this subfamily include mineralocorticoid receptor (MR), progesterone receptor (PR), androgen receptor (AR), and estrogen receptor (ER). These members share analogous protein 3D structures and recognize a very similar DNA element. In particular, MR and PR are the members closest to GR, and the ligand cross-interaction of these receptors are the main cause for off-target effects of GCs such as hypertension (blood pressure) and water retention (19). Therefore, we examined the off-target effects of our GCs on those receptors in the reporter assay at its saturation concentration of 1 μM. For MR activity, VSG156, VSG158, and VSG159 have a lower activity than corticosterone and DEX, similar to FF, but higher than FP (Fig. 2*A*). For PR activity, VSG158, VSG159, FP, and FF have similar activities as progesterone (Fig. 2*B*). For AR and ER, all of the tested GR ligands show little activity (Fig. 2 *C* and *D*).

Gene Expression and Pathway Analyses of Highly Potent GCs. We then used microarrays to profile the gene expression patterns of the GCs VSG158 and VSG159, in parallel with FF and DEX, in mouse macrophage RAW264.7 cells (Gene Expression Omnibus ID GSE119789, ref. 20). We used lipopolysaccharide (LPS) to elicit the inflammation and then treated with various GCs to investigate their antiinflammatory activities. Aligned with DEX, from most down-regulated genes to most up-regulated genes, VSG158, VSG159, and FF followed the overall same trend as DEX (Fig. 3*A*). The Venn diagrams show that genes induced or repressed by VSG158, VSG159, FF, and DEX highly overlap with each other. The number of genes repressed by VSG158, VSG159, FF, and DEX (more than twofold) are 696, 637, 562, and 575, respectively, and more than half of these (365) are commonly repressed by all four GCs. Similarly, the number of

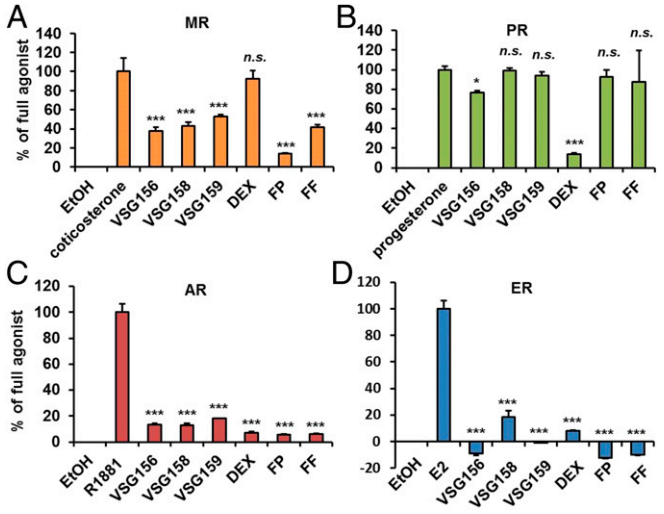

Fig. 2. The off-target activities of GCs at the saturation centration of 1 μM in AD293 cells. (*A*) MR reporter activity. (*B*) PR reporter activity. (*C*) AR reporter activity. (*D*) ER reporter activity. Error bars indicate SD; $*P < 0.05$; $***P < 0.001$; n.s., not significant; one-way ANOVA analysis with a Tukey test; $n = 3$.

genes induced by VSG158, VSG159, FF, and DEX (more than twofold) are 660, 675, 787, and 659, respectively, and more than half of these (395) are commonly induced by all of these GCs (Fig. 3*B*). Pathway analysis of the common genes regulated by VSG158, VSG159, FF, and DEX show that the top repressed pathway is the cytokine–cytokine receptor interaction pathway (Kegg pathway # 04060) and the top induced pathway is pyrimidine metabolism (Kegg pathway # 00240) (*SI Appendix*, Table S1). This is consistent with our previous analysis of VSGC12 (14). Since the cytokine–cytokine receptor interaction is the key pathway that regulates the cellular inflammatory response (21), and its repression is the major target for antiinflammatory effects, we further examined the details of the repression activity on this pathway. A close look at commonly repressed genes from this pathway, normalized to DEX, shows that VSG158, VSG159, and FF have a stronger (two- to eightfold) repression activity than the standard GC DEX (Fig. 3*C*) on the majority of those genes, including repression of the key proinflammatory cytokines IL1β, IL1α, and TNFRSF9.

In Vivo Activity of GCs in an Ovalbumin-Induced Asthma Mouse Model. We next utilized a mouse model of ovalbumin (OVA)-induced acute asthma (22) to assess the potency of these compounds. To mimic the inhalation method for human asthma treatment, we intranasally delivered our treatments. We first compared the effects of VSG158, VSG159, and VSGC12 at a relatively high dose of 0.125 mg/kg. The data show that at this dose all compounds, including VSG156, can effectively repress the airway hyper-responsiveness (AHR) to the basal level (Fig. 4*A*). Particularly, VSG158 showed a robust repression that was even lower than the basal level, and VSG159 and VSG156 also showed a stronger repression than VSGC12. Since VSG158 showed superior repression activity, we determined a full dose effect curve for VSG158 in this model in comparison with FF, the most potent clinical GC for asthma treatment. As before, VSG158 at 0.125 mg/kg showed full repression (≥100%) of AHR, while FF at 0.125 mg/kg showed a 95% repression. A further eightfold decrease of the VSG158 concentration (0.015635 mg/kg) still showed a higher repression (96%) than FF at 0.125 mg/kg (Fig. 4*B*). On the other hand, an only twofold decrease of the FF dose (0.0625 mg/kg vs. 0.125 mg/kg) caused a dramatic decrease of activity, suggesting that VSG158 is at least eight times more potent than FF in the mouse asthma model. Finally, we further lowered the VSG158 dose 10 times (0.0125 mg/kg) and 20 times (0.00625 mg/kg) compared with that of FF (0.125 mg/kg). In addition, we also used the same dose of VSG159 as comparison. Our data show that even at 0.0125 mg/kg, VSG158 still displayed the same repression as FF at 0.125 mg/kg (Fig. 4*C*), suggesting that VSG158 is 10 times more potent than FF in this model. Of note, VSG159 at 0.0125 mg/kg showed substantial repression of AHR, but was less potent than VSG158 at the same dose of 0.0125 mg/kg and FF at 0.125 mg/kg. We also examined the effects of VSG158, VSG159, and FF on differential cell counts. Different from previous high-dose treatment of VSGC12 and FF in the mouse asthma model via the i.p. delivery method, the very low dose of intranasally delivered VSG158 (0.0125 mg/kg), VSG159 (0.0125 mg/kg), and FF (0.125 mg/kg) did not show a significant effect on the differential cells count (*SI Appendix*, Fig. S1*A*). Similar results were obtained in the OVA IgE and histology examination (*SI Appendix*, Fig. S1 *B* and *C*). We reasoned that the lung function assay (AHR) is much more sensitive to the dose of inhaled GCs than the differential cell counts and plasma IgE level, which may need a higher dose or longer period to promote the difference.

Antiinflammatory Effects of VSG158 in Steroid-Susceptible and Steroid-Resistant Airway Inflammation. Asthmatic inflammation is characterized by infiltration of various inflammatory cells into the bronchoalveolar lavage (BAL) and lung. We and others previously demonstrated that adjuvants used for antigen sensitization determine the types of inflammatory responses in the

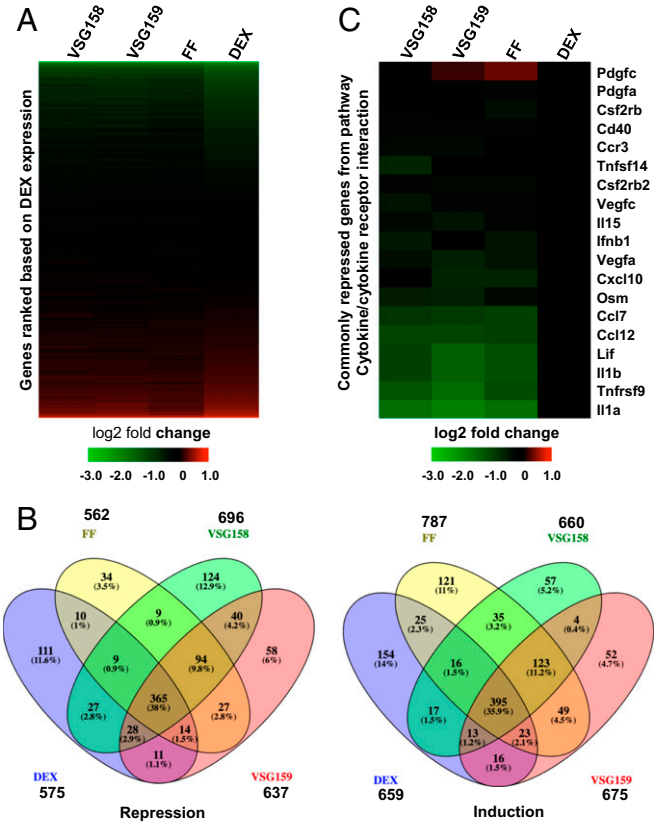

Fig. 3. Microarray analysis of gene expression changes in response to GCs. (*A*) Gene profiling of the effects of VSG158, VSG159, FF, and DEX in inflammation-induced (LPS treatment) mouse macrophage RAW264 cells. Data were plotted as expression levels relative to vehicle (DMSO) and aligned to the gene expression pattern seen upon DEX treatment from most down-regulated to most up-regulated genes. (*B*) Venn diagrams of genes induced or repressed more than twofold in RAW264.7 cells. (*C*) Gene expression profile of commonly repressed genes from the cytokine–cytokine receptor interaction pathway in RAW264.7 cells. Data were normalized to DEX.

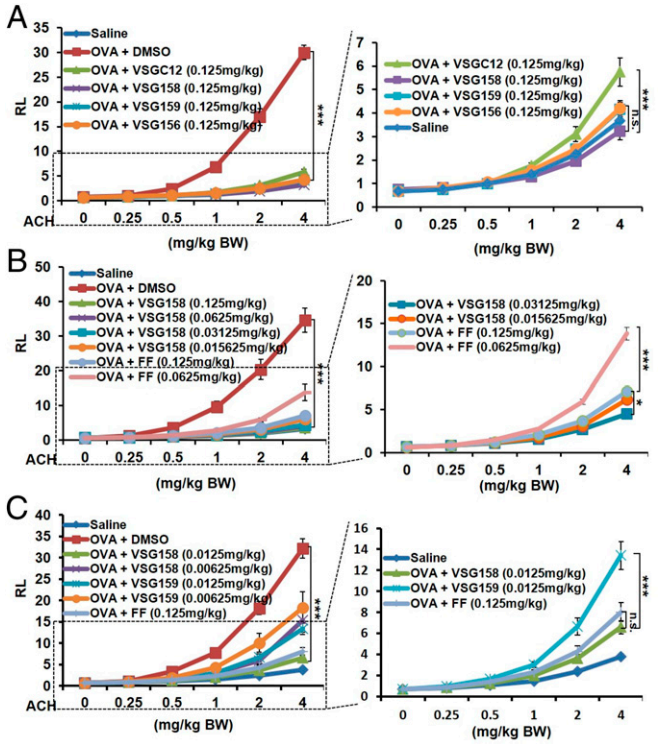

Fig. 4. Examination of the treatment effect of GCs in a mouse asthma model. (*A*) Examination of the treatment effect of GCs on lung-function AHR at the relatively high dose of 0.125 mg/kg via intranasal delivery method. (*B*) A comparison of VSG158 and FF at different doses by the intranasal delivery method. (*C*) A comparison of VSG158, VSG159, and FF at very low dose via the intranasal delivery method. Error bars indicate SEM. *P* values are shown for the 4-mg ACH/kg BW data points and were calculated by two-way ANOVA analysis with a Bonferroni post test ($n = 10$): $*P < 0.05$; $***P < 0.001$; n.s., not significant; $n = 8$–10. ACH, acetylcholine; BW, body weight; RL, resistance of lung (centimeters H_2O per second per milliliter).

airway (23, 24). For example, antigen sensitization in alum adjuvant induces predominantly eosinophil infiltration associated with Th2-type effector CD4 T cell responses. By contrast, antigen sensitization in Complete Freund's Adjuvant (CFA) induces neutrophilic infiltration with effector CD4 T cells expressing Th17/Th1 phenotypes. Importantly, neutrophilic airway inflammation displays steroid-resistant properties as seen in severe asthmatic patients who are refractory to steroid treatment (25, 26). Since VSG158 has higher GR-binding affinity and potently suppresses AHR, we next tested if it could suppress steroid-resistant inflammatory immune responses.

Using the cockroach antigen (CA)-induced inflammation model that we recently reported (23), we sensitized mice with CA in alum adjuvant to induce steroid-susceptible inflammation (Fig. 5*A*). Intraperitoneal injection of DEX (2.5 mg/kg) was chosen based on a previous study that investigated steroid-resistant inflammation (24). VSG158 (0.0125 mg/kg) was injected i.p. during intranasal CA challenge. DEX at a 200-fold higher concentration (2.5 mg/kg) was included as a GC control. Both DEX and VSG158 significantly diminished eosinophil infiltration in the BAL, although VSG158 was superior in reducing both proportion and absolute numbers of infiltrating eosinophils (Fig. 5*B*). Lung-infiltrating CD4 T cell production of inflammatory cytokines was also significantly reduced by GC treatment (Fig. 5*C*). Moreover, histopathologic examination further supported the data obtained by flow cytometry analysis (Fig. 5*D*). Of note, VSG158 achieved better antiinflammatory effects at a two orders of magnitude lower dose than DEX. We then switched the model system to neutrophilic inflammation, a steroid-refractory inflammation, induced by sensitizing mice with CFA instead of alum (Fig. 5*E*). Unlike alum-induced inflammation, neutrophil and CD4 T cell infiltration in the BAL was pronounced in this model (Fig. 5*F*). DEX treatment had no effect on downregulating inflammatory cell infiltration in the BAL, consistent with the steroid-resistant phenotype as reported previously (24). Likewise, FF injected at 0.125 mg/kg also failed to reduce inflammatory responses. However, VSG158 injected at 0.0125 mg/kg substantially diminished inflammatory cell infiltration in the BAL and lung accumulation of effector CD4 T cells expressing inflammatory cytokines (Fig. 5*G*). Lung histopathologic examination also supported these results (Fig. 5*H*). Therefore, higher potency of VSG158 enables it to suppress steroid-resistant inflammation in the lung.

Side Effects of GCs. Major side effects of GCs include childhood growth inhibition, metabolic syndrome, and bone loss. We examined the effects of VSG158, VSG159, FF, and DEX on these categories at their minimal concentrations sufficient to fully repress AHR and eosinophilic/neutrophilic inflammatory responses. To test the effects of those GCs on the weight gain of growing young mice, 7-wk-old DBA/1 mice were treated with daily intranasal delivery of VSG158 (0.0125 mg/kg), VSG159 (0.0125 mg/kg), FF (0.125 mg/kg), and DEX (2.5 mg/kg) for 2 wk. No significant weight loss was observed in VSG158, VSG159, and FF groups. In contrast, we observed a significant weight loss in the DEX group (Fig. 6*A*). We note that body weight loss does not necessarily correlate with growth inhibition, that the harmless effect of VSG158 on body weight loss is only suggestive, and that the exact effect of VSG158 and VSG159 on growth (i.e., body length) velocity needs to be further investigated. GC-induced metabolic syndrome includes obesity, high blood sugar, and high blood pressure, and insulin resistance is one of the keys to trigger those events. We first measured the fasting blood sugar level of 7-wk-old male BALB/c mice treated with various GCs for 2 wk via intranasal delivery. The data show that DEX and VSG158 do not increase the blood glucose level compared with vehicle control while VSG159 and FF slightly increase the fasting blood glucose level (*SI Appendix*, Fig. S2*A*). To investigate the possibility of insulin resistance, we then measured the fasting plasma insulin level of those mice. To our surprise, all GCs increased the plasma insulin level in the BALB/c mice (*SI Appendix*, Fig. S2*B*) with FF showing the strongest effect. A calculation of HOMA-IR shows that VSG158 and VSG159 had an effect similar to that of DEX while FF showed the strongest increase of HOMA-IR (Fig. 6*B*). Lymphoid atrophy is a general effect of GC treatment and sometimes is considered to be an undesired effect of GC treatment. VSG158 (0.0125 mg/kg), VSG159 (0.0125 mg/kg), and FF (0.125 mg/kg) treatment did not cause a significant reduction of spleen size, while DEX (2.5 mg/kg) caused a dramatic shrinkage of the spleen in DBA/1 mice (Fig. 6*C*). Bone loss is another major adverse effect of GC. By X-ray microcomputed tomography, we examined the bone microarchitecture of femurs from the mice treated with different GCs. DEX caused a significant decrease in the average object area-equivalent circle diameter per slice and cross-sectional thickness in cortical bone, while VSG158, VSG159, and FF did not significantly alter those parameters (Fig. 6*D*). Similarly, in trabecular bone, while DEX decreased both the bone volume/tissue volume ratio and trabecular thickness, the other treatments did not cause a significant change in those parameters (Fig. 6*E*).

Pharmacokinetic Properties of GCs. Enhanced lung inflammation repression activity and minimal side-effect profile of the GCs make them good candidates for clinical asthma treatment. We thus decided to examine their preclinical pharmacokinetic (PK) properties. We first examined the PK profile of VSGC12, VSG158, and VSG159 via oral and i.v. administration (*SI Appendix*, Table S2). For oral administration, the plasma concentrations of these compounds reached their peaks all within 2 h, and the T_{max} for VSGC12, VSG158, and VSG159 were 2.0, 1.0, and 1.3 h, respectively. The half-lives for VSGC12, VSG158, and VSG159 were 3.7, 5.3, and 7.5 h, respectively. The bioavailabilities

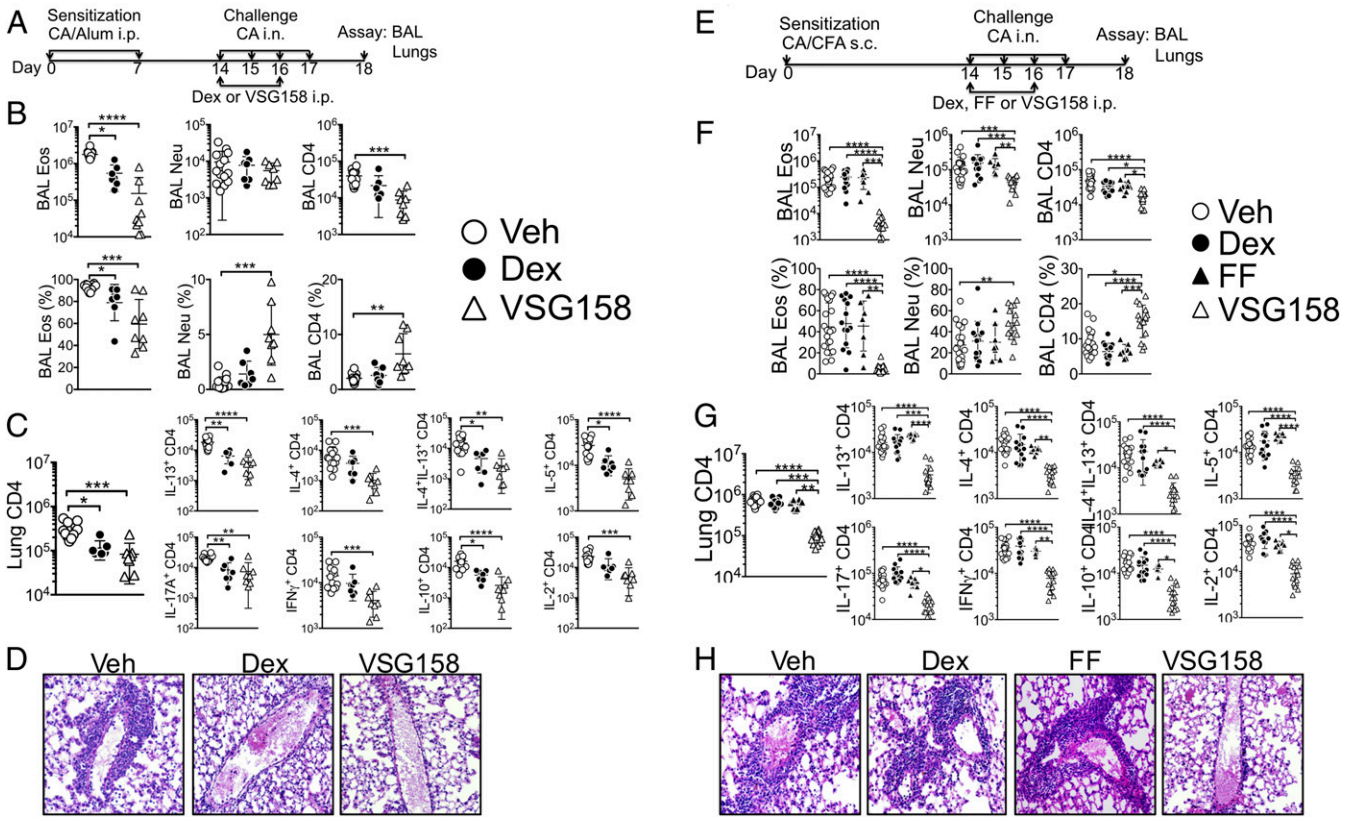

Fig. 5. Treatment of eosinophilic and neutrophilic airway inflammation with various GCs. (*A–D*) Steroid-susceptible inflammation model. (*A*) Experimental schedule. Vehicle, Dex, or VSG158 were intraperitoneally injected. (*B*) Upon sacrifice, BAL cells collected were examined for eosinophils, neutrophils, and CD4 T cells. (*C*) Lung cells were ex vivo stimulated, and intracellular cytokine expression was determined by FACS analysis. (*D*) Histopathology. Magnification: 20×. (*E–H*) Steroid-resistant inflammation model. (*E*) Experimental schedule. Vehicle, Dex, FF, or VSG158 were intraperitoneally injected. (*F* and *G*) Cellular responses were measured as described above. (*H*) Histopathology. Magnification: 20×. Each symbol represents an individually tested mouse from more than three independent experiments. Error bars indicate SD; $*P < 0.05$; $**P < 0.01$; $***P < 0.001$; $****P < 0.0001$; one-way ANOVA analysis with a Kruskal–Wallis test followed by a Dunn's test; $n = 8–21$.

for VSGC12, VSG158, and VSG159 were 42.4, 17.7, and 8.3%, respectively, suggesting that the design of –O- or –S- esters to substitute the nonhydrolyzable nitro group at the C-21 position does indeed decrease stability. However, compared with the superior bioavailabilities of FP and FF (1 and 1.5%, respectively), these numbers remain still high, suggesting that the ester groups are only partially hydrolyzed in liver. For the i.v. administration, the half-lives for VSGC12, VSG158, and VSG159 were 4.8, 6.0, and 5.7 h, respectively. The kinetics curves of these compounds after i.v. or oral administration are shown in *SI Appendix*, Fig. S3. Since VSG158 has the highest potency in repressing lung AHR and lung inflammation in the mouse model, we also profiled VSG158 via the intranasal delivery method at different doses (*SI Appendix*, Table S3). VSG158 reached the peak in plasma concentration after about 1–2 h at different doses. When the distribution of VSG158 and VSG159 was examined between lung and circulation following intranasal delivery, both compounds predominantly distributed in the lung rather than in the circulation (*SI Appendix*, Fig. S4), suggesting that both compounds have excellent lung retention properties, which is ideal for inhaled GCs. However, we need to point out that the excellent lung retention does not necessitate the ideal treatment in lung as inhaled GCs are regulated by multiple factors in the lung, such as pulmonary clearance, metabolism, and absorption. For example, the inhaled GC may be brought back to the GI track by mucociliary and cough clearance because of the size of the inhaled particle (>6 μm) (27) and thus increase systemic availability of the inhaled GC. On the other hand, lung is known to express a battery of primary detoxification enzymes, such as a member of the cytochrome P450 (CYP) family, and metabolic enzymes including epoxide hydrolase and esterases; therefore, the lung retention time also depends on the expression level of those enzymes (27). The complete and comprehensive PK properties of these GCs need to be thoroughly determined.

Discussion

VSG158 was designed with the rationale of introducing an ester group at the C-21 position of the VSGC12 backbone to deactivate this potent GR ligand by hepatic metabolism. Surprisingly, substitution of the *O*-fluoromethyl carbothioate group increased the potency of VSG158 more than 10 times above that of the currently most potent clinical GC, FF, in the mouse asthma model, making it the most potent GC for asthma treatment. The superior antiinflammatory activity enables VSG158 to deliver the same treatment effect as FF at only 1/10 of FF's dose. Importantly, at the effective dose tested (0.0125 mg/kg, >96% repression of lung AHR), VSG158 did not express significant side effects on body weight loss and bone loss. Interestingly, VSG158 did not increase fasting blood glucose level, but had a mild effect in increasing the fasting plasma insulin level like DEX in male BALB/c mice; this is different from our previous study of female DBA/1 mice under a nonfasting condition, which may be due to experimental setting (sex, strain, and fasting). Nevertheless, VSG158 still shows better HOMA-IR value than the clinically most effective FF under the current setting. While FF displays a slightly higher GR affinity (Fig. 1*E*), VSG158 has a better transrepression/transactivation ratio in cell-based reporter assays (Fig. 1 *C* and *D*) and has higher efficacy in repressing

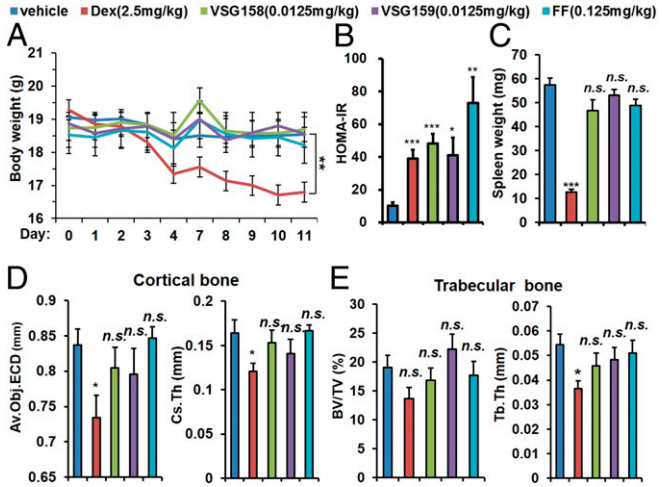

Fig. 6. Examination of the side effects of intranasally delivered GCs in designated animals with 2 wk of treatments at indicated doses. (*A*) Body weight loss of DBA/1 mice. Body weights were monitored daily for 12 d. (*B*) HOMA-IR of male BALB/c mice. Blood samples were collected at day 14. (*C*) Spleen size of DBA/1 mice. Spleen samples were collected at day 14. (*D*) Cortical bone average object area-equivalent circle diameter (Av.Obj.ECDa) per slice and cross-sectional thickness (Cs.Th) of DBA/1 mice. Cortical bone samples were collected at day 14. (*E*) Trabecular bone, bone volume/tissue volume ratio (BV/TV), and trabecular thickness (Tb.Th) of DBA/1 mice. Trabecular bone samples were collected at day 14. Error bars indicate SEM; $*P < 0.05$; $**P < 0.01$; $***P < 0.001$; n.s., not significant; one-way ANOVA analysis with a Tukey test; $n = 5–6$.

AHR in the mouse asthma model. It is especially intriguing to find that VSG158 was highly efficient in downregulating neutrophilic airway inflammation, a model considered steroid-resistant inflammation, which remained unaffected when treated with DEX or FF. The cellular mechanisms underlying the efficacy remains to be determined.

In summary, we have developed an extremely potent GC, VSG158, which to our knowledge is the only GC that can reverse steroid-resistant asthma in a mouse model. This GC displays the highest potency that we have ever seen in repressing lung AHR and lung inflammation in a mouse model of eosinophilic and neutrophilic airway inflammation. It is 10 times more potent than the most potent clinical GC, FF, and is capable of delivering the treatment effects at a dose that does not elicit major side effects of GC. VSG158 also has acceptable PK properties and a favorable lung/circulation distribution after intranasal delivery, suggesting that this GC is important to investigate in research on the clinical treatment of asthma.

Materials and Methods

All animal studies were approved by the Institutional Animal Care and Use Committees of Van Andel Institute, University of California, San Francisco, and Cleveland Clinic Foundation. Detailed methods about cell-based reporter assays, in vitro GR ligand-binding assay, microarray analysis of gene expression and animal studies, including an OVA-induced mouse asthma model, CA-induced airway inflammation model, intranasal delivery method, mouse body weight measurement, spleen and bone collection, bone density examination, plasma glucose and insulin measurement, as well as pharmacokinetics studies are described in *SI Appendix, Materials and Methods*.

Statistical Analysis. Statistical analyses were based on the sample type and experiment setting. For mouse lung-function assays, the readouts of which are influenced by both challenge dose and treatments, two-way ANOVA analysis with a Bonferroni post hoc analysis was applied. Note that the *P* values shown in Fig. 4 refer to the highest challenge dose (acetylcholine: 4 mg/kg), i.e., vary only by one factor, which is treatment. We therefore also performed a one-way ANOVA analysis with Tukey post hoc analysis, which yielded similar results as the two-way ANOVA analysis. Data were log-transformed for normality and equal variance. For other experiments that were affected only by treatments, one-way ANOVA analysis with a Tukey test or Kruskal–Wallis test (Fig. 5) were applied. See figure legend for the statistical analysis for each assay.

Database. The microarray data were deposited in the National Center for Biotechnology Information Gene Expression Omnibus database under accession no. GSE119789 (20).

ACKNOWLEDGMENTS. We thank the Vivarium and Transgenic Core of the Van Andel Institute for help and assistance in the animal studies; Zach Madaj (Van Andel Institute Bioinformatics and Biostatistics Core) for consultation on statistical data analysis; and Parker W. de Waal (Van Andel Institute) for instruction on using the R program for multiple statistical analysis. This study was supported by an American Asthma Foundation Fund 2010 Senior Award and 2017 Extension Award; by a Proof of Concept Innovation Award from the Van Andel Institute; by National Natural Science Foundation of China Grants 91217311 and 81502909 (to H.E.X.); by the Van Andel Research Institute (H.E.X.); and by National Institute of Allergy and Infectious Diseases/NIH Grants AI125247 and AI121524 and an American Asthma Foundation 2014 Senior Award (to B.M.).

1. Murphy SL, Xu J, Kochanek KD (2013) *Deaths: Final Data for 2010*. National Vital Statistics Reports (Centers for Disease Control and Prevention, Atlanta), Vol 61, No 4.
2. Holgate ST (2010) A look at the pathogenesis of asthma: The need for a change in direction. *Discov Med* 9:439–447.
3. Crompton G (2006) A brief history of inhaled asthma therapy over the last fifty years. *Prim Care Respir J* 15:326–331.
4. Tamm M, Richards DH, Beghé B, Fabbri L (2012) Inhaled corticosteroid and long-acting β2-agonist pharmacological profiles: Effective asthma therapy in practice. *Respir Med* 106(Suppl 1):S9–S19.
5. Holgate ST, Polosa R (2006) The mechanisms, diagnosis, and management of severe asthma in adults. *Lancet* 368:780–793.
6. Ernst P, Suissa S (2012) Systemic effects of inhaled corticosteroids. *Curr Opin Pulm Med* 18:85–89.
7. Lipworth BJ (1999) Systemic adverse effects of inhaled corticosteroid therapy: A systematic review and meta-analysis. *Arch Intern Med* 159:941–955.
8. Syed YY (2015) Fluticasone furoate/vilanterol: A review of its use in patients with asthma. *Drugs* 75:407–418.
9. O'Byrne PM, et al. (2014) Efficacy and safety of once-daily fluticasone furoate 50 mcg in adults with persistent asthma: A 12-week randomized trial. *Respir Res* 15:88.
10. McKeage K (2014) Fluticasone furoate/vilanterol: A review of its use in chronic obstructive pulmonary disease. *Drugs* 74:1509–1522.
11. Villa E, Magnoni MS, Micheli D, Canonica GW (2011) A review of the use of fluticasone furoate since its launch. *Expert Opin Pharmacother* 12:2107–2117.
12. He Y, et al. (2014) Structures and mechanism for the design of highly potent glucocorticoids. *Cell Res* 24:713–726.
13. Suino-Powell K, et al. (2008) Doubling the size of the glucocorticoid receptor ligand binding pocket by deacylcortivazol. *Mol Cell Biol* 28:1915–1923.
14. He Y, et al. (2015) Discovery of a highly potent glucocorticoid for asthma treatment. *Cell Discov* 1:15035.
15. Crim C, Pierre LN, Daley-Yates PT (2001) A review of the pharmacology and pharmacokinetics of inhaled fluticasone propionate and mometasone furoate. *Clin Ther* 23:1339–1354.
16. Salter M, et al. (2007) Pharmacological properties of the enhanced-affinity glucocorticoid fluticasone furoate in vitro and in an in vivo model of respiratory inflammatory disease. *Am J Physiol Lung Cell Mol Physiol* 293:L660–L667.
17. Derendorf H, Hochhaus G, Meibohm B, Möllmann H, Barth J (1998) Pharmacokinetics and pharmacodynamics of inhaled corticosteroids. *J Allergy Clin Immunol* 101:S440–S446.
18. Biggadike K, et al. (2009) Design and x-ray crystal structures of high-potency nonsteroidal glucocorticoid agonists exploiting a novel binding site on the receptor. *Proc Natl Acad Sci USA* 106:18114–18119.
19. Frey FJ, Odermatt A, Frey BM (2004) Glucocorticoid-mediated mineralocorticoid receptor activation and hypertension. *Curr Opin Nephrol Hypertens* 13:451–458.
20. He Y, Liu H, Xu HE (2019) Gene expression profiling of novel glucocorticoids for severe asthma in RAW264.7 cells. Gene Expression Omnibus. Available at https://www.ncbi.nlm.nih.gov/geo/query/acc.cgi?acc=GSE119789. Deposited September 11, 2018.
21. van der Meer JW, Vogels MT, Netea MG, Kullberg BJ (1998) Proinflammatory cytokines and treatment of disease. *Ann N Y Acad Sci* 856:243–251.
22. Chen C, Huang X, Sheppard D (2006) ADAM33 is not essential for growth and development and does not modulate allergic asthma in mice. *Mol Cell Biol* 26:6950–6956.
23. Jang E, et al. (2017) Lung-infiltrating Foxp3$^+$ regulatory T cells are quantitatively and qualitatively different during eosinophilic and neutrophilic allergic airway inflammation but essential to control the inflammation. *J Immunol* 199:3943–3951.
24. McKinley L, et al. (2008) TH17 cells mediate steroid-resistant airway inflammation and airway hyperresponsiveness in mice. *J Immunol* 181:4089–4097.
25. Wang M, et al. (2016) Impaired anti-inflammatory action of glucocorticoid in neutrophil from patients with steroid-resistant asthma. *Respir Res* 17:153.
26. Guiddir T, et al. (2017) Neutrophilic steroid-refractory recurrent wheeze and eosinophilic steroid-refractory asthma in children. *J Allergy Clin Immunol Pract* 5:1351–1361.e2.
27. Olsson B, et al. (2011) *Pulmonary Drug Metabolism, Clearance, and Absorption* (Springer, New York).